JOURNAL OF MATERIALS SCIENCE **35** (2000) 1589–1596

Direct observation of frictional seizure of mild steel sliding on aluminum by X-ray imaging

Part I *Methods*

M. CHANDRASEKARAN, A. W. BATCHELOR, N. L. LOH
School of Mechanical and Production Engineering, Nanyang Technological University, Singapore 639798
E-mail: mcmargam@ntu.edu.sg

Many of the mechanical or metallurgical failures originate from subsurface cracks or changes in microstructure of the materials. It would be quite informative to material scientists to view the changes below the surface while testing to get a direct evidence of the mechanisms claimed to be governing a particular process like dislocation movement/grain boundary sliding, crack opening displacement, wear, stress concentration etc. In this work, we have used an X-ray microscope for *in-situ* observation of interfacial features during the friction and wear testing of mild steel specimens sliding against Al 6061 disk. This technique enables the observation of interfacial features of the hidden contact. Multiple tests were conducted at different sliding speeds of 2, 4 and 5 m/s. The images obtained during the tests indicated the presence of various sub surface processes such as adhesive transfer, stress fields, island formation and roughening. Wear was also found to be concentrated over a certain specific area during the initial part of the test but later the contact developed into a conformal contact following a lumpy transfer of material.

1. Introduction

Direct observation of sub surface features during a dynamic test has been difficult and was restricted by the extent and the quality of observation possible with the conventional tools such as Scanning Electron Microscope (SEM) or a optical (CCD) camera [1–7]. Earlier theories on the mechanisms of friction and wear of sliding systems tested using a pin on disk assembly were mostly based on the post test analysis of the disk and pin surfaces which lacked direct evidences for the same. Conducting *in-situ* tests in a SEM (Scanning Electron Microscope) or a CCD camera overcame this lacuna. This again was restricted to the observation of leading and trailing edges of the contact. Spikes *et al*. viewed the sliding interface during sliding using a sapphire disk sliding against a steel specimen using a TV Camera and infrared emission radiometry [8, 9]. This experiment enabled identification of the hidden process of wear in a special case, but could not be extended to other cases. In order to overcome this, it was essential to use a technique, which could reveal the interfacial reactions/mechanics during sliding in an non-idealized sliding contact. Real time radiography or X-ray imaging, as it is popularly known, has the capability of observation of interfaces in non-idealized sliding contacts [10–12]. This overcomes the previously described limitations. The X-rays pass through the sample and the disk and hits a fluorescent screen, which in turn re-emits visible light radiation whose intensity depends on the intensity of X-rays striking the screen. The present work involves *in-situ* observation of frictional seizure in a tribo-meter located in a microfocus X-ray microscope and the parallel measurement of friction wear rate. The present work is also aimed at gaining a better understanding of the interfacial process during sliding.

2. Experimental

Experiments were performed using a custom built pin on disk apparatus. A 2 HP motor was used to drive the aluminum disk which was used as a counterface and the pin surface henceforth referred to as specimen was supported on a holder with a provision for the X-ray head can be lowered to stay very close to the specimen surface. Aluminum was selected as the disk material for two reasons namely 1) it is increasingly used in weight saving applications and 2) to minimise the loss or attenuation of X-rays after passing through the contact. The specimen holder was fitted onto a beam structure with provisions for sensing the experimental parameters such as friction force, displacement, temperature close to the contact and the oxygen potential surrounding the testing atmosphere. A FeinFocus X-ray microscope with a beam spot size of 4–20 μm diameter was used in all experiments. The schematic representation of the apparatus and the image processing system is provided in Fig. 1. Steel pins of dimension ϕ 5 mm $\times$ 3 mm thick specimens were polished using a 1000 grit SiC

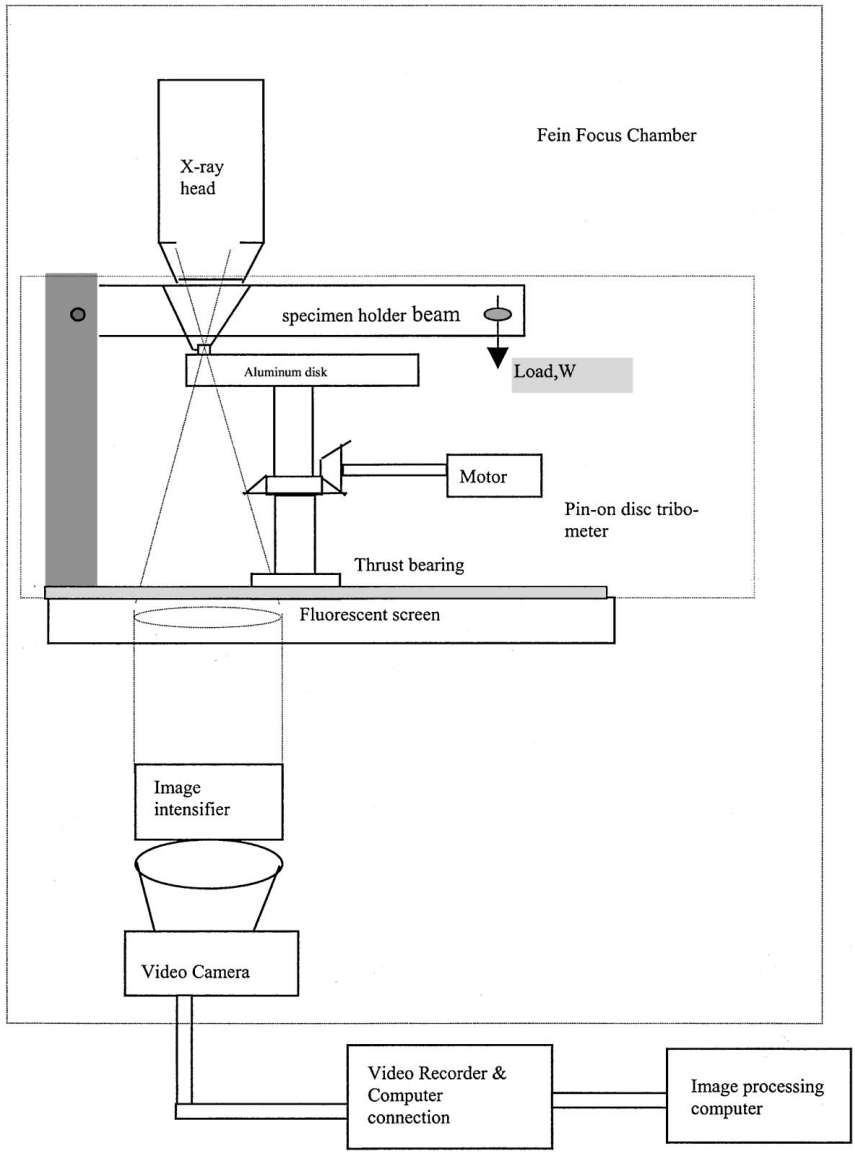

Figure 1 Schematic representation of the test apparatus and the image processing system.

abrasive paper to provide a surface roughness value of Ra 0.03–0.05 μm and was fixed to specimen holder designed to facilitate X-ray observation. The counterface disks were made of Al 6061 machined and fine turned to the roughness value of 0.04–0.06 μm Ra value with a skewness and kurtosis of 1.7 and 3.4 respectively. The wear and seizure experiments were carried out at different sliding speeds of 2, 4 and 5 m/s. The events during the wear and seizure was closely followed on by X-ray imaging on a fluoroscopic screen which was passed through a 1st order recursive filter. The filtered images were recorded continuously in a video tape which was replayed and images were freezed at the definite intervals of time and image processing was carried out to remove noise signals from the image.

3. Results

Figs 2–4 show the successive X-ray fluoroscopic images of the steel specimen sliding on aluminum 6061 disk. Fig. 2a, the control X-ray fluoroscopic image of the MS pin/Al disk interface. It can be observed from the control image that the surfaces were relatively free of any defects and had an almost smooth surface. The light intensity variations on the projected image can be possibly taken as a representation of the relative surface roughness. This is because of the fact that the X-rays get attenuated/absorbed differentially by the discontinuities in the specimen surface. It is a well know fact that the specimen surface consists of peaks and valley's no matter how best it is polished. The presence of peaks in the specimen surface first contacts the surface of the disk. These peaks either deform or plow into the disk surface depending on the hardness difference inherent between the specimen and disk material. This leads to a conformal contact between the disk surface and the pin surface. As the X-ray penetrates through the contact thus established it gets differentially absorbed depending on the density variations. That is to say the X-ray intensity received after penetrating through the peak of specimen and those received after penetrating through the valley of the specimen are different. A corresponding mapping of peaks and valley are produced if a histogram of intensity profile is taken. Spreading of the contact is inferred wherever the line profile is flatter in the control image. A representative histogram

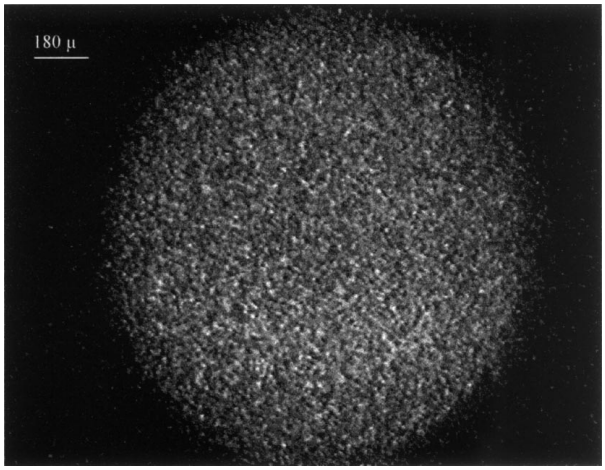

(a)

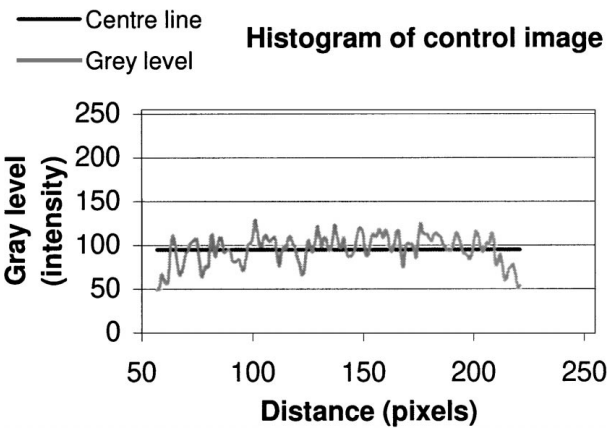

(b)

Figure 2 (a) Control X-ray Fluoroscopic image of the MS/Al interface tested at 2 m/s sliding speed; (b) histogram along the centre line of control X-ray fluoroscopic image of MS pin/disk tested at 2 m/s.

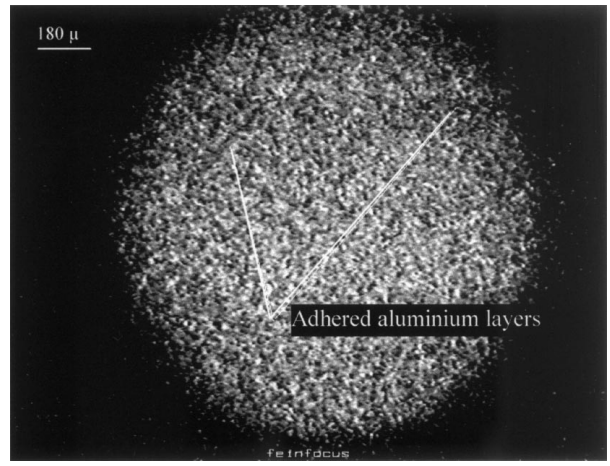

(a)

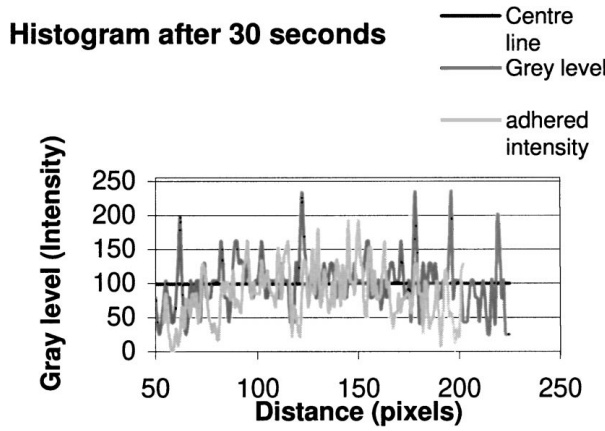

(b)

Figure 3 (a) X-ray Fluoroscopic image of the MS/Al interface tested at 2 m/s sliding speed after 30 seconds; (b) histogram of image along the centre line, ater 30 seconds of sliding at 2m/s.

line profile is shown in Fig. 2b taken along the horizontal centre line of the image. The control image also shows spreading of contact due to the localised high loads on the asperity contacts. The jagged appearance of the image is essentially due to the spreading of the contact.

Fig. 3a taken relatively at an early stage of sliding after 30 seconds indicate further asperity truncation and transfer of Al from the disk surface to the steel with a friction coefficient of 1.19. A possible cause of this early friction rise may be the high solubility of Al in Fe of about 22% [10–12]. Fig. 3b, which shows the representative histogram profile along the horizontal centre line with superposed line profile along the pointers of adhered intensity revealed that the profile pattern was of similar nature to the control image except for the differences in magnitude. The transfer of Al and adhesion to steel surface was evident from the reduction gray levels in the image over isolated region separated by a darker line. The difference in gray level is due to transfer and accumulation of material accounting for higher attenuation/absorption of X-rays resulting in regions with lower gray level.

Fig. 4a show the interface of sliding during seizure. This shows a considerable increase in the size of plateau thus formed and extensive plowing may be the cause of seizure with little effect by bonding of transfer layers to the parent metal. Fig. 4b shows the representative histogram profile along the horizontal centre line of the image and superposed line profile taken through the region where bonding and mechanical locking was claimed. The mechanical locking is evident from the large fluctuations in the intensity levels from 0–255 (indicative of black-to-bright white spot). Bonding is inferred from regions showing full attenuation of X-rays. Full attenuation is possible only when the density of material interposed in the contact is higher than the density of disk material which absorbs the X-rays thus producing a black region (zero gray level).

4. Discussion

Since X-rays get differentially absorbed in the specimen due to the changes in the specimen during the test, the transmitted X-ray intensity suffers similar variational effects, which is reflected back on the visible light image developed on the screen. The images developed on the fluorescent screen was captured using a high speed digital camera with a shutter speed of 500 frames/seconds attached to the microscope and the associated noise in the image was filtered using a synoptic recursive filter to get a noise filtered image on the screen. This was further processed to highlight certain important changes during sliding governing the mechanism of the wear process. The X-ray intensity was fixed

at 76 kV and the current density was 53 μA for focusing the X-ray beam approximately at the interfacial layer. The images were collected at specified intervals of time and 1 minute was the typical period between observations to monitor the changes in real-time. The main purpose being observing the images with the progress of wear and also to identify the driving mechanism of seizure at a particular position. The images were then mask processed using median function to eliminate spikes in gray levels due to random noise and the resultant image was analyzed for changes along each row of the matrix the image in digitized form is a matrix of 512×512 pixel matrix with the pixel intensity (gray values) as the elements. Thus the above process leaves us with a image matrix and any changes occurring in the matrix gray levels, after the filtering and image processing sequence, can be attributed to the changes in X-ray path length at those points with reasonable confidence level. Unlike the normal NDT methods where one single process is being viewed without any influence by other mechanisms here an effort has been made to view the wear mechanisms which is a combination of multiple mechanisms with a particular mechanism being dominant at a point of time [13–16].

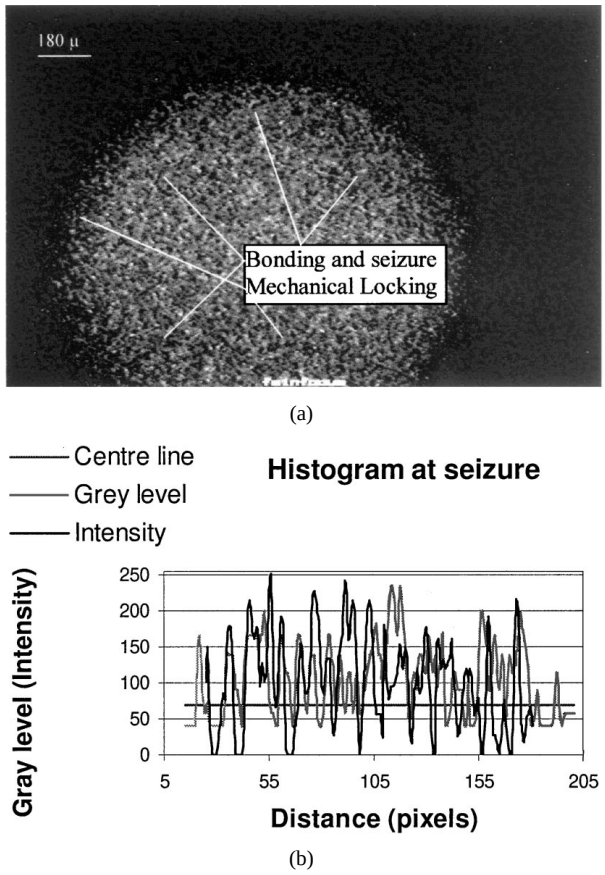

Figure 4 (a) X-ray Fluoroscopic image of the MS/Al interface tested at 2 m/s sliding speed at seizure; (b) histogram of image along the centre line, at seizure tested at 2m/s.

4.1. Interpretation methods

The basic principle on which the X-ray operates is absorbency of the individual atoms in the material. In passing through the specimen, the X-ray radiation is differentially absorbed due to the changes in thickness of the specimen or presence of any contaminants in the X-ray path. The present work is done with the assumption that the materials used are free from any internal defects and interface is free from contaminants at the start of the test. Thus any changes occurring in the image is only by wear and associated mechanisms. In order to make sure that the assumptions are correct a control X-ray fluoroscopic image is obtained for each of tests followed by continuous recording of the images during the tests. Any changes occurring during sliding is reflected back on the fluoroscopic image, which is captured using a CCD camera. The images captured is fed through a computer which digitizes the image into a $512 * 512$ pixel matrix. This pixel matrix

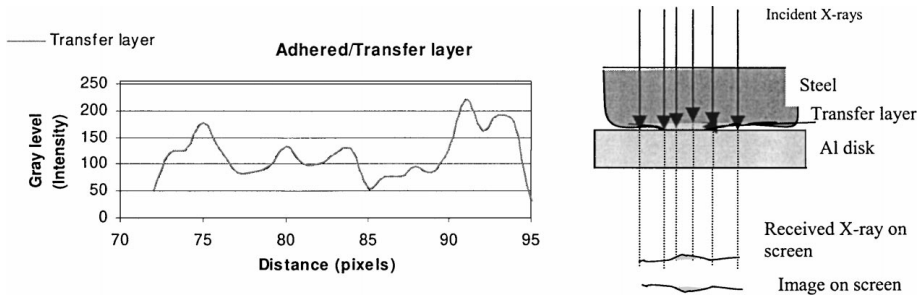

Figure 5 Histogram profile and the schematic representation of transfer film/adhered layer.

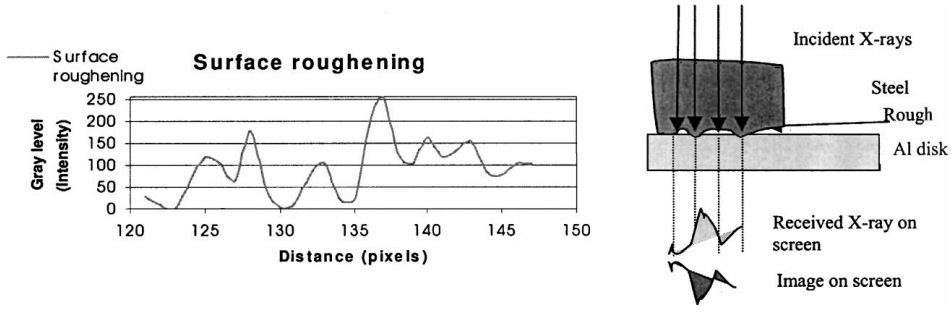

Figure 6 Histogram profile and the schematic representation of surface roughening effect.

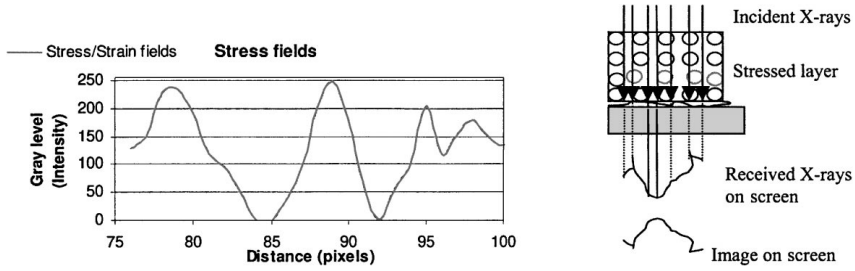

Figure 7 Histogram profile and the schematic representation of strain fields.

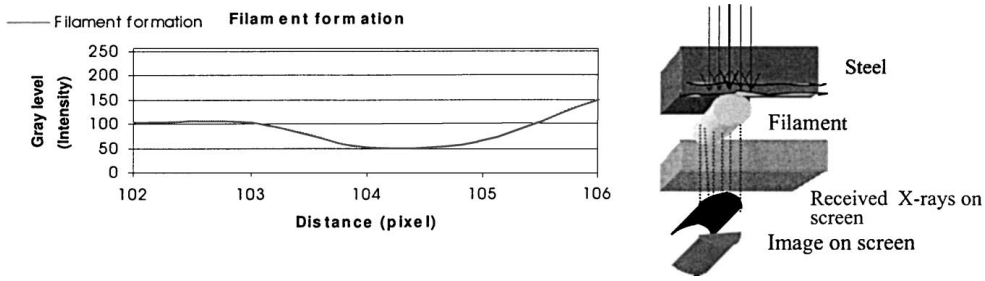

Figure 8 Histogram profile and the schematic representation of filament formation.

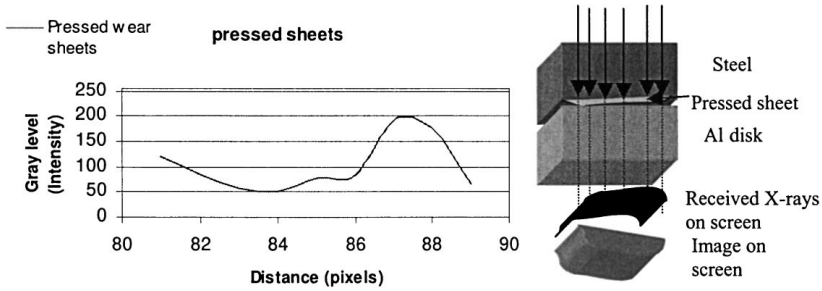

Figure 9 Histogram profile and the schematic representation of pressed/extruded wear sheets.

is reconstructed back as an analog image in the TV screen. The main advantage of this digitization is that it can identify changes in the image matrix elements which otherwise may not be visible to the human eye. The matrix is composed of gray levels of picture elements. The term gray level is used here to quantify the intensity of visible light in the image, i.e., a gray level of 0 means that there is no visible light and a gray level of 255 represents bright white light. The intermediate values between 0–255 represent the combination of white and black colour at different ratios to represent the details of the image. The obtained images are further processed to make the significant changes obvious which otherwise is invisible on the TV monitor.

The changes in the image matrix are due to the inherent processes associated with the wearing-in of materials. The literature's on tribology have so far listed the possible existence of transfer, mechanical locking, inter-metallic formation, roughening and bonding during sliding in process from the post test analysis of worn specimens [17, 18].

4.2. Transfer/adhered layer

Transfer is a process in which a small layer of material is removed from one of the sliding surface and gets attached to the other surface of the tribo pair. Essentially the transferred layer does not have a constant thickness and varies over the length of the transferred material. This is identified in the X-ray image as a gradual lowering of gray levels to a mean value followed by a gradual increase in gray levels to the average gray values of the image in the area of transfer. This is due to the fact that the X-ray intensity is optimized to focus at the interface and any changes occurring at the interface is clearly reflected as changes in gray levels. Moreover the disk surface rotates at a high speed and the effects of disk thickness variations are subtracted by applying a median function to the image obtained. This leaves us with the significant changes in the images at the interface of the specimen alone. The transfer effect is depicted in the above histogram, which was taken from the same images in which transfer was claimed.

4.3. Roughening

Similarly a roughening can be identified by a sharp variation in gray levels at neighboring points in a image as roughening always results in production of peaks and valley on the surface of the specimen. This means that the contact would be established between a peak on the pin surface and disk and valley will not have a contact with the disk surface at that instance of imaging. Thus air gap would be produced between the valley and disk surface which does not restrict the X-ray path, whereas on the other hand the X-ray passing though the peak to disk and on to fluoroscopic screen suffers from a greater loss of X-ray intensity.

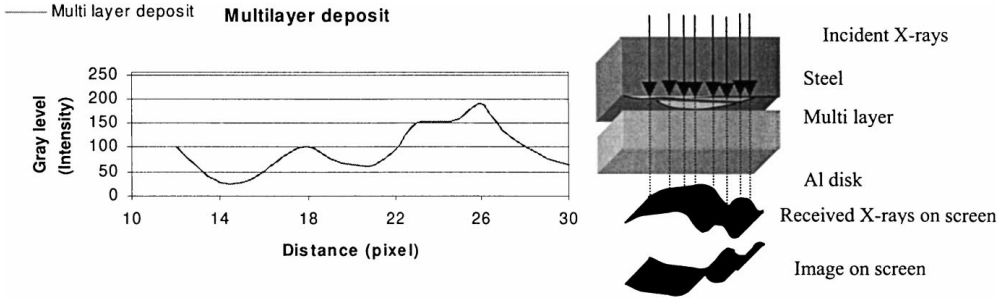

Figure 10 Histogram profile and the schematic representation of multi-layer deposit.

So there would be a significant difference in the gray levels of neighboring points and will be reproduced as a dark and white spot combination in neighboring points in the image. When clustering of such combination occur it is termed as surface roughening.

4.4. Stress/strain fields

The stress fields either results in clustering of atoms at a particular sight or changes the inter-atomic distance depending upon the magnitude of stress whether it is compressive or tensile. Depending on the changes in inter-atomic spacing the absorbency of X-ray will vary. These variations are normally reflected back on the X-ray image as patches having different gray levels (darker) compared to the other parts of the image with no boundary line separating from the rest of the areas [13].

4.5. Filament formation

During sliding the wear particles often are rolled to form a cylinder. The formation of cylindrical shape on the sliding surfaces are termed as filaments formation. This can be identified in the X-ray image as a drop in gray levels having a inverted curve shape. This finds its explanation in the fact the distance traversed by the X-ray along the diametrical chord of the filament is higher where it suffers higher loss of X-ray and it changes gradually to normal average gray level over the thickness of the filament. Thus if a line profiles across the filament is taken it produces an inverted curve shape in the histogram which is interpreted as filament formation.

4.6. Pressed sheets

In case of the pressed sheets the histogram profile is similar to the transfer film except for a slight variation in the profile. In case of transfer film, the histogram profile reflects a gradual decrease and increase in gray levels. For the pressed sheets which is a resultant effect of transfer film being compacted to form a sheet of uniform thickness, the histogram profile is shallow has a sharp gradient of increase/decrease in gray levels. The histogram below depicts the typical histogram profile of pressed/extruded sheets.

4.7. Multi-layer deposit

Multiple layer deposition on one of the surfaces takes place while wearing-in due to adherence of pressed wear debris on to one of the surfaces. This multi layer deposit can be identified from observing the histogram profile, which resembles a step. This depicted in the histogram give below (Fig. 10) and this was used for identifying multi layers in the fluoroscopic images.

4.8. Layer peel off

Layer peel off is a process wherein the adhered layer/a thin layer of base material is removed from the surface of the specimen at contact. Unlike transfer where, a sheet of material from the counterface adheres to the specimen surface, a layer of material, which originally was adhering to the specimen, is removed from the specimen surface. Hence, there is an increase in the gray levels as the material is removed from the surface of specimen, which is stationary. The histogram profile appears similar to transfer layer but is inverted. That is to say that there is a gradual increase in gray levels followed by a fixed gray level and a gradual decrease in gray levels to average value. This is depicted in the histogram profile given below (Fig. 11).

4.9. Islands

Islands are regions where a lump of material is removed during sliding process leaving behind a depression on the surface of the specimen. This is more severe form of

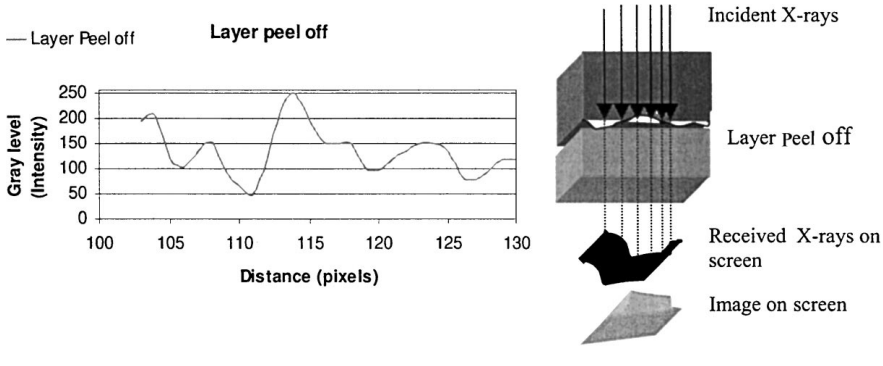

Figure 11 Histogram profile and the schematic representation of layer peel off.

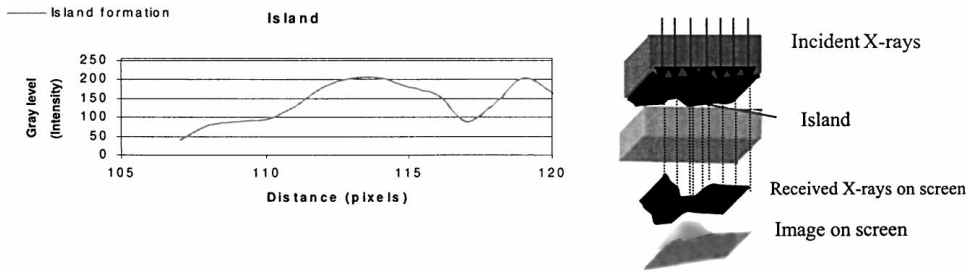

Figure 12 Histogram profile and the schematic representation of island formation.

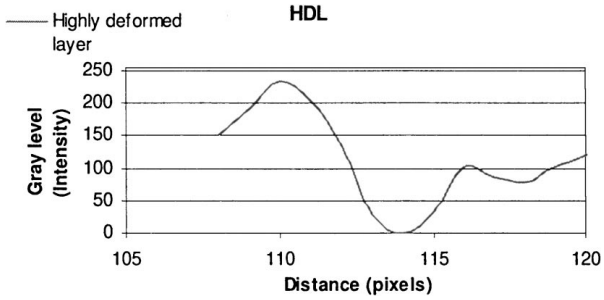

Figure 13 A typical histogram profile of a highly deformed layer.

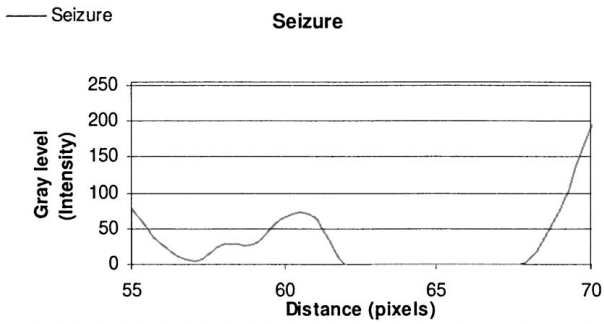

Figure 14 A typical histogram profile of a seized contact showing no transmission of X-rays in the bonded region.

material removal and often results in mechanical locking of sliding surfaces resulting in seizure of the sliding component. Since this is a severe form of layer peel off the histogram profile is similar to layer peel off except for a steep gradient in gray level differences. This principle was used to identify island formation in sliding contacts. A typical histogram profile of an island formation is given below.

4.10. Highly deformed layer

Dry sliding often leads to accumulation of stress fields over a time period leading to formation of a highly deformed layer. This layer is similar to the stress fields explained earlier in this chapter except that a larger area is affected instead of a localized atomic disorder due to stress. Histogram profile given below shows a typical nature of a highly deformed layer image.

4.11. Bonding and seizure

If bonding occurs between the surfaces it results in formation of an alloy or an inter-metallic depending on the phase diagrams of the particular combination of materials. This alloy/inter-metallic always has densities different from those of the materials in combination and can be calculated by applying rule of mixtures depending on the percentages of materials. The areas that are bonded can be identified as patches similar to the one observed in transfer in the X-ray images. But the areas have a lower gray level as compared to transfer, since in transfer the material having lower density is transferred and is identified as lighter area bounded by a line of lower gray level as opposed to dark patches in the case of bonding. Histogram below depicts the histogram of a bonding/seizure, which does not allow any transmission of X-rays through the contact.

4.12. Melting

Melting wear occurs when the flash temperature at the sliding contact exceeds the melting point of one of the contacting surfaces. The process of incipient melting of surfaces can be inferred from the fluoroscopic image if the gray levels are at maximum over a distance, i.e., at 255 over a pixel distance of 5 or more [15].

5. Conclusion

A pilot study of dry sliding contact between aluminum and steel where an X-ray microscope enabled in-situ observations of the sliding contact provided evidence for the following conclusions.

1. By applying the principle of radiography and image processing various subsurface phenomena can be identified during sliding.
2. Wear was chaotic and yet had cyclic behaviour as identified from the profile of the histograms at different stages of sliding.
3. Sliding speed was found to have considerable effect on the mechanism of seizure of mild steel in dry contact.
4. The reduction in gray levels of the image to zero and rapid fluctuations in gray level over isolated areas indicate the imminence of seizure in dry contacts.

Acknowledgements

The authors gratefully acknowledge the support of Nanyang Technological University by sponsoring the research project ARP 67/93.

References

1. W. HOLZHAUER and S. J. CALABRESE, *ASLE Transactions* **30**(3) (1987) 302.
2. S. GUNSEL, H. A. SPIKES and M. ADERIN, *STLE Tribology Transactions* **36**(2) (1993) 276.

3. K. HOKKIRIGAWA, in "Surface Modification Technologies VIII," edited by T. S. Sudarshan, and M. Jeandin (The Institute of Materials, 1995) p. 93.
4. T. KATO, K. HOKKIRIGAWA, T. FUKUDA, M. SHINOOKA and J. TAKAHASHI, in "Surface Modification Technologies X," edited by T. S. Sudarshan, K. A. Khor and M. Jeandin (The Institute of Materials, 1997) p. 841.
5. W. A. GLAESER, *Wear* **73** (1981) 371.
6. S. J. CALABRESE, F. F. LING and S. F. MURRAY, *ASLE Trans.* **26**(4) (1983) 455.
7. Y. TSUYA, K. SAITO, R. TAKAGI and J. AKAOKA, in Proc. of Int. Conference on Wear of Materials, Dearborn, Michigan, April 1979 (ASME New York, 1979) p. 57.
8. J. ENTHOVEN, H. A. SPIKES, *Tribology Transactions* **39**(2) (1996) 441.
9. J. C. ENTHOVEN, P. M. CANN and H. A. SPIKES, *STLE Tribology Transactions* **36**(2) (1993) 258.
10. R. HALMSHAW, "Non-destructive Testing" (Edward Arnold, London, 1987) p. 16.
11. R. HALMSHAW, "Industrial Radiology: Theory and Practice" (Applied Science Publishers, New Jersey, 1982).
12. R. HALMSHAW, in "Proc.4th European Conf. NDT," edited by J. M. Farley and R. W. Nichols (Pergamon Press, Oxford, 1988) Vol. 1, p. 139.
13. W. HARTMAN, in "Real Time Radiologic Imaging: Medical and Inductrial Applications," ASTM Special Technical Publication 716, edited by D. A. Garrett, and D. A. Bracher (American Society for Testing of Materials, Philadelphia, 1980) p. 201.
14. R. E. BURGE, A. G. MICHETTE and P. J. DUKE, "X-ray Microscopy and X-ray Imaging, Vol. 1: Scanning Microscope," (1987) p. 891.
15. J. CHIKAWA, in "Real Time Radiologic Imaging: Medical and Inductrial Applications," ASTM Special Technical Publication 716, edited by D. A., Garrett and D. A. Bracher (American Society for Testing of Materials, Philadelphia, 1980).
16. I. FRUMKIN, A. NOTEA and A. BRESKIN, NDT&E International **27** (1994) 317.
17. L. H. CHEN and D. A. RIGNEY, *Wear* **136** (1990) 223.
18. KATSUZO OKADA, *Japanese Journal of Tribology* **39**(5) (1994) 529.

Received 28 September 1998
and accepted 22 July 1999